2026 IEEE International Conference on Robotics and Automation (ICRA 2026)
June 1-5, 2026. Vienna, Austria

Error Fields: personalized robotic training to enhance movement accuracy across speed

Bruno Borghi[1,2], Naveed Reza Aghamohammadi[1,2], Adriana Cancrini[1,2], Arturo Ramirez[1,2], Courtney Celian[2], James L. Patton[1,2]

***Abstract*— We developed a personalized robotic training paradigm called Error Fields, which learns the user mistakes during an upper-limb reaching task and generates perturbations that drive the subject's trajectories toward greater precision. We hypothesized that force fields pushing the limb toward regions of largest error tendencies would intensify practice, accelerating motor adaptation and improving the speed and accuracy of the subject's movements. To test this hypothesis, we analyzed error reduction across the experiment by comparing groups that received Error Fields with those subjected to traditional Error Augmentation and a null-force control condition. In all conditions, participants were additionally exposed to a curl field to simulate motor impairment. Error Fields showed improved accuracy post-training and induced after-effects once the force was removed, demonstrating promising benefits for investigation in a post-stroke population.**

I. INTRODUCTION

Robotic technologies have the potential to support neurorehabilitation by providing continuous monitoring of patient performance and enabling repetitive high-intensity practice, which is critical for motor learning and recovery, but varies widely between individuals [1], [2]. Most robotic frameworks remain limited in their ability to customize therapy to individual patient's impairments, abilities, and recovery trajectory resulting in too generic treatments [3]–[6]. Rehabilitation outcomes depend on interventions tailored to the specific needs of each patient; thus, developing effective frameworks first requires identifying individual impairments [7]–[9] and assessing the individual's sensitivity to movement errors [10].

One such approach that builds on this individualized framework is error augmentation (EA), a technique that visually or haptically increases movement errors to facilitate motor re-learning across a variety of tasks including upper extremity rehabilitation [11]–[16]. In our previous work, we have expanded on this concept by augmenting the errors that participants most frequently make [17]–[19]. This novel approach, named Error Fields (EF) training, targets and alters individual error patterns by first building a distribution model of each participant's movement errors as they occur and then designing a customized intervention that selectively amplifies those specific error tendencies. Preliminary evidence suggests that EF training leads to greater improvements in motor re-learning than conventional EA interventions [17]. Despite its promise, EF training has not yet been tested in three-dimensional (3D) movements, where natural variability in arm trajectories plays an important role [20], [21]. In fact, only a handful of studies [5], [22] have examined robotic treatments under 3D life-like conditions. Motivated by these open questions, we investigated how Error Field training induces motor adaptation in upper limb movements. To this end, we specifically introduced three distinct types of force during the experiment described in detail below.

- *Curl force field*. Velocity-dependent perturbation designed to distort the trajectory of natural movements and emulate the speed-dependent motor impairments found in the post-stroke population [23].
- *Error Augmentation force (EA)*. Perturbing force that amplifies the hand's position error by a fixed multiplication factor [11].
- *Error Field force (EF)*. Force based on the subject's trajectory errors, where the robot first identifies hand deviations from the ideal path and then applies force according to the error distribution. The EF paradigm operates on the principle that emphasizing errors enhances learning more effectively than directly correcting them [14].

II. METHODS

A. Experimental Apparatus

We used the Barrett® Upper-Extremity Robotic Trainer (BURT®) [24], a robotic arm with three-degrees-of-freedom designed for upper-limb motor training (Fig 1). It provides real-time, 3D haptic feedback and force rendering, allowing for natural and unrestricted upper-extremity movements. This robotic system delivers torque through a unique cable transmission system to allows remote placement of motors in the housing while delivering end effector force, reducing distal weight and allowing backdrivability. The low inertial cable-driven design ensures high-fidelity force transmission and precise control of limb dynamics [25]. The system features a large, adjustable range of motion and an intuitive user interface, facilitating accessibility and consistency between sessions.

The 100% of the research reported in this publication was supported by the National Institute of Neurological Disorders and Stroke of the National Institutes of Health under award number R01NS053606 ($2,717,005 total project costs) financed with Federal money. The content is solely the responsibility of the authors and does not necessarily represent the official views of the National Institutes of Health.

[1] Richard and Loan Hill Department of Biomedical Engineering, University of Illinois Chicago, Chicago, IL, USA. nagham2@uic.edu, acancr2@uic.edu, aramire4@uic.edu

[2] Robotics Lab at Center for Neural Plasticity, Shirley Ryan AbilityLab, Chicago, IL, USA. bborghi@sralab.org, ccelian@sralab.org, jpatton@sralab.org

The robot interfaces with a custom augmented reality system called LookinGlass (Fig. 1 A) used to increase immersion [26]–[28]. The system consists of two vertically stacked panels, a 3D stereoscopic display that generates images, reflected to a semi-silvered mirror lower panel, allowing the participant to see-through their real hands and arms interacting with the robot below the mirror surface. The participants wear active shutter glasses to see in stereoscopic 3D. A real-time graphic interface, developed in Unity®, communicated directly with the BURT® system to ensure synchronized visual and haptic feedback. Depth perception was further enhanced through multiple monocular depth cues incorporated in the graphical scene, including perspective, occlusion, shadows, relative height, and texture gradients [29]. The calibration procedures aligned the virtual scene to each participant's viewpoint by adjusting seating position and head alignment relative to the LookinGlass system and stereoscopic camera within Unity®. This ensured that the visual representation of the cursor is spatially consistent with the participant's actual hand position throughout the task.

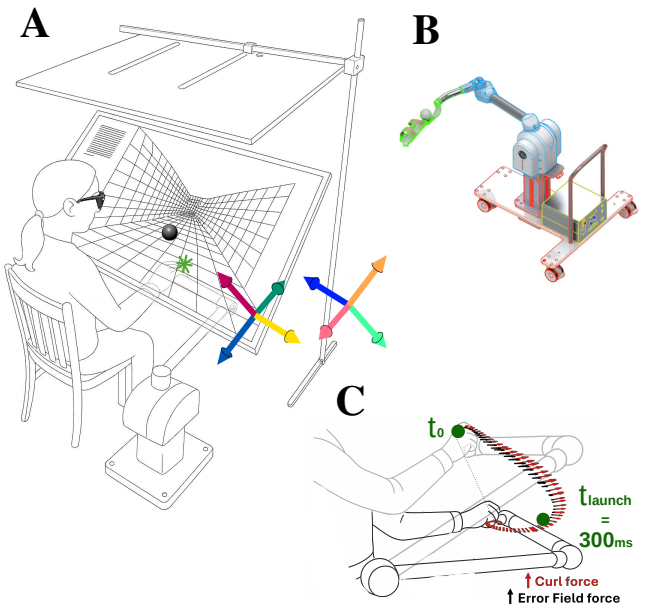

Fig. 1. Experimental setup. A) Participant holding the robotic handle of the BURT system while performing the reaching task displayed on the LookinGlass 3D screen, wearing 3D glasses. The green asterisk on the screen is the virtual cursor, driven by the subject's hand, and the grey sphere is an example of a virtual target. The eight possible movement directions performed during the experiment are illustrated by the colored arrows displayed next to the screen. B) Model design of the BURT robot, from Barrett Medical™ BURT® user manual. C) Example of a reaching trial in which the subject's arm movement is perturbed by robot-generated forces: the curl force (red) is applied throughout the entire movement, while the Error Field force (black) is applied only during the first 300 milliseconds (launch).

B. Protocol

Each participant completed the experimental session in one visit, for a total duration of one hour and a half, and was randomly assigned to one of three treatment groups during training (refer to section C for details). Group 1 received Error Field force (EF), Group 2 received Error Augmentation force (EA), and Group 3 received a null treatment (SHAM). Participants used the BURT® robotic handle to control a cursor on the screen and complete repeated 10-cm reaching movements toward spherical targets, with a diameter of 2 cm (Fig.1 A). Participants were given 5 seconds to complete each reaching task, after which the system automatically advanced to the next target. Target positions followed a constrained random-walk pattern to ensure that participants encountered a wide variety of arm positions. Four specific directions, termed *practiced*, are repeatedly presented throughout most of the experiment. To evaluate generalization of motor learning, additional trials include reaching toward *unpracticed* directions, defined as the opposites of the *practiced* directions (see colored arrows in Fig. 1 A). A color-based visual feedback at the target indicated whether the participant's peak launch speed fell within the desired range of 0.28–0.44 m/s. This range was determined from aggregated pilot data, based on the magnitude of the velocity-dependent curl force applied during movement. Throughout movement, robot-generated forces were applied to the participant's arm to introduce controlled perturbations (Fig.1C). Across the sessions, participants performed a total of 735 reaches, which included both practiced and unpracticed directions. To minimize fatigue, they took short rest breaks after every 20 movements. The experimental session consisted of the following nine phases:

- *Familiarization* (43 movements). The subjects first familiarized themselves with the experimental environment and the robotic interface. They performed reaching movements in the practiced directions, without any external forces applied. Data collected during this phase were excluded from subsequent analysis.
- *Unpracticed Pre-Training Force On* (42 movements). Subjects completed reaching movements in unpracticed directions. A curl force was intermittently applied, perturbing one randomly selected trial out of every five, while the remaining four remained unperturbed.
- *Pre-Training Force Off* (21 movements). Subjects completed reaching movements in the practiced directions without any external forces applied. These trials were included to assess baseline error levels before training.
- *Pre-Training Force On* (210 movements). Participants performed in the practiced directions with the intermittent curl force. For each perturbed trial, movement errors were profiled within the first 300 milliseconds according to both direction and time. These data informed the construction of a time-dependent, three-dimensional multivariate Gaussian distribution of errors for each unpracticed direction, as described in [17], yielding an ensemble statistic of error patterns under force-field perturbation.
- *Training* (336 movements). Subjects reached in practice directions with the curl force present while an additional training force vector was applied during the first 300 milliseconds of movement. The specific characteristics

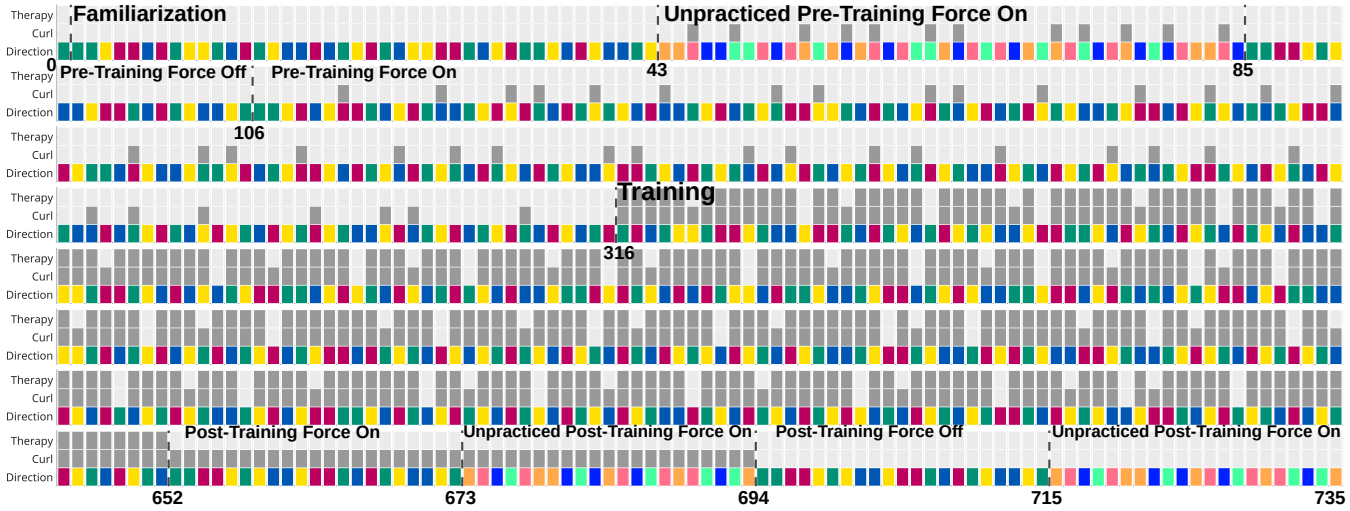

Fig. 2. Experimental protocol showing the sequence of movement trials divided into the nine different phases described in Methods - Section B. Protocol. The x-axis shows the movement number (or trial), progressing from 0 to 735, the total number of trials. Each color block encodes the movement directions, following the color-coding in the arrows of Fig 1. On top of each one, there are blocks indicating what experimental condition was turned on in that trial, where semi-transparent means no force, one gray block means curl force on while two gray blocks indicate curl force plus the therapy force (EF or EA).

of this force depend on the experimental condition to which each participant was assigned (EF, EA or SHAM. See Methods, Section C). Two catch trials are present in this phase, one where the treatment force is removed and the other where no forces are applied.

- *Post-Training Force On* (21 movements). Subjects reached in the practiced directions while the curl force field was applied on every trial.
- *Unpracticed Post-Training Force On* (21 movements). Subjects reached in the unpracticed directions while the curl force field was applied on every trial.
- *Post-Training Force Off* (21 movements). Subjects performed reaching movements in the practiced directions with no forces applied.
- *Unpracticed Post-Training Force Off* (21 movements). Subjects performed reaching movements in the unpracticed directions with no forces applied.

C. Experimental Conditions

Participants were randomly assigned to one of the three conditions designed to compare the specific effects of Error Augmentation (EA) and Error Fields (EF) with a control treatment (SHAM). To calculate the EA and EF perturbations, we defined an error vector $\mathbf{e}(\delta)$ based on three different measurements:

$$\mathbf{e}(\delta) = \begin{bmatrix} \mathbf{e}_{ext}(\delta) \\ \mathbf{e}_{hor}(\delta) \\ \mathbf{e}_{ver}(\delta) \end{bmatrix}$$

The three components of the error vector are defined in the error reference frame *[E]* (see Fig. 6), with δ denoting the path distance, as defined in [30]. Horizontal $\mathbf{e}_{hor}(\delta)$ and vertical $\mathbf{e}_{ver}(\delta)$ errors represent the instantaneous distances of the hand position from the ideal straight line connecting the start and target positions. Extent error $\mathbf{e}_{ext}(\delta)$, instead, is defined as the difference between the ideal hand position, based on Flash and Hogan's minimum jerk profile [31], and the projection of the actual hand position onto the ideal line, see [18]. Further details on the computation of these error components are provided in APPENDIX A. The three conditions are outlined below:

- *Error Field force (EF).* The force was derived from the subject's own trajectory errors. Once the robot has studied the error tendencies, it applies forces to push the hand in those regions. This approach was based on the principle that amplifying movement errors during training facilitates motor learning more effectively than directly compensating for them [17]. The resulting force is formally expressed as:

$$\mathbf{F}_{EF}(\delta) = \lambda p(\delta)\mathbf{e}(\delta)$$

  where λ is a direction-dependent constant corrective gain such that the overall force applied to the subjects hand never exceeds 20 N and $p(\delta)$ is the Gaussian probability distribution of error vector (see [17]).
- *Error Augmentation force (EA).* The applied force haptically amplifies instantaneous movement errors and is defined as:

$$\mathbf{F}_{EA}(\delta) = \gamma\mathbf{e}(\delta)$$

  where γ is a constant number [17].
- *SHAM*. In this condition (null training), no additional force to the curl force field was applied to the subject.

Whether in the EF or EA group, the treatment force is always paired with the curl force field.

D. Subjects Enrollment

Twenty-seven subjects (10 males and 17 females, aged 27 ± 9 years, 26 right-handed, 1 left-handed) participated

in the study, with a total of 9 participants assigned into each of the three groups. Inclusion criteria required participants to be 18 years or older, with no history of stroke, and be able to provide informed consent. Individuals were excluded from the study if they had severe medical conditions; upper extremity impairments that affected movement, range of motion, strength, or coordination; or visual deficits that interfered with their ability to complete the study. The Northwestern University Institutional Review Board (Chicago, IL) approved this study (STU00215000) and reliance was established with the University of Illinois at Chicago research ethics authority (STUDY2021-1108). All participants provided written informed consent in adherence to the Declaration of Helsinki.

E. Data analysis

The output of every subject's experiment is a dataset of 735 files, one for each trial, containing the movement data information, including time, current experiment phase, condition, treatment type, target position, velocities, exerted forces and trajectory errors. The data were then analyzed in Matlab (MathWorks, Inc., Natick, MA). The main focus was on the error amplitude, that keeps track of the hand's deviation from the ideal trajectory based on the minimum jerk profile [31] [32], and the perpendicular error, illustrated in Fig 6. Particularly, we prioritized the launch phase, which is the first 300 milliseconds from the movement onset, visible in Fig 1 between the t_0 and t_{launch}, in order to focus on the feed-forward control of the movement and prevent the feedback corrections. To avoid skewing results computing the averages with near-zero values at movement onset, it was considered in the analysis only the maximum value of the errors. A decrease in error across the trials under the presence of forces would support the motor adaptation hypothesis, reflecting improved accuracy with practice, while an increase in the error when the forces are removed, would indicate a residual compensatory strategy adopted by the nervous system to counterbalance the perturbations, known as aftereffects. The statistical analyses performed involved a paired t-test and a non-parametric Kruskal-Wallis test, with a 95% confidence interval and an α value of 0.05.

III. Results

Our results indicate that subjects trained with the Error Fields force experienced the highest accuracy improvement across speed for the curl force field phases, and after-effects when the forces were turned off, this difference can be seen respectively in the red and yellow dots in Fig 3. The Error Augmentation group also showed similar results during the pre- and post-training phases with the curl force applied. However, unlike the Error Field group, they showed a lower accuracy improvement and exhibited no after-effects once the force was removed, as indicated by the non-negative yellow distribution in Fig 3, meaning the accuracy has increased even after the force was turned off. Additionally, the increase in accuracy observed during curl force trials compared to force-off trials is significantly larger for the Error Field group and Error Augmentation group compared to the SHAM, suggesting a stronger and significant induced motor change in subjects exposed to these two treatments. The analysis is based on the correlation between error and speed distributions, to help extrapolate more the error variations in the really low mistakes movements that characterize the neurotypical population, really hard to detect otherwise. The results obtained reinforce our hypothesis of a higher induced motor adaptation when a person is exposed to a bigger and personalized external force, the Error Field force, particularly when compared to the Error Augmentation group, which exposes the subjects to a similar condition with the only difference of not adjusting the force to their error tendencies, but simply amplify it by a constant value. Higher improvements are also seen when compared to the SHAM group, where only the curl force was applied and no noticeable changes were present across the phases.

Analyzing a different metric in Fig 4, the maximum perpendicular error, we were able to break down the analysis to visualize the direct effects of the curl force field. In particular, the gray area in the figure represents the distribution of how much the first exposure to the force changed the participant's accuracy across speed. This is an essential step as it constitutes the starting point where an initial increase of error is induced in the subject, in order to then have it corrected throughout the experiment. It can be visualized that the direct effects have significantly higher accuracy reduction compared to each subject's baseline accuracy, as shown by the gray violin plots distance from zero. The same results for direct effects were also found in Fig. 3 when considering all subjects together, not shown in the plots, and in the EF group only when divided into groups.

A following analysis has been done on the motor adaptation during training with the EF and EA force, which compares the accuracy before and after the Training phase, so in a situation when on top of the curl force field a second force was applied to the subject's hand. In these analysis, in the red violin plots in Fig 4, we can notice how the Error Fields and Error Augmentation force are all good disturbances in generating a higher accuracy improvement when coping with the curl force. Also in the SHAM group, which has not been exposed to any additional disturbance than the curl force, a positive accuracy shift is present, as expected when a long practice session with a viscous Coriolis force promotes motor adaptation [23]. Between all of these performance refinements, only the EF and EA effects are significantly higher than zero (no Improvement Area) in both metrics analyzed, supporting the hypothesis of greater and individualized external forces that elicit enhanced motor adaptation. At the same time, unexpected results are given by the pre- vs post-Training force off phases, where no evidence of after-effects is seen as the force off (yellow) distributions are mostly positive, differently from what we obtained from the maximum error amplitude analysis figure.

We also looked at how distributions of error changed between the treatment groups, i.e. we tried to answer if the subjects' habits changed either during the treatment or afterward.

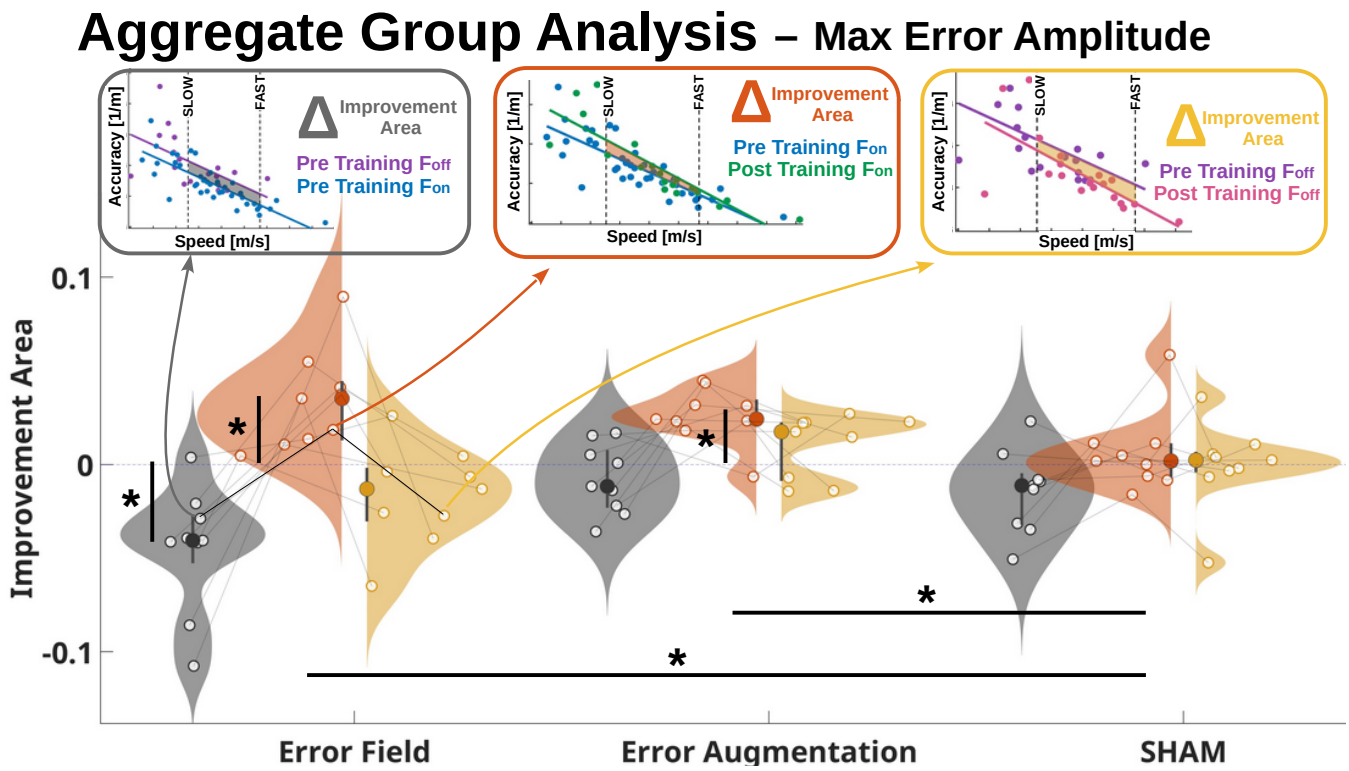

Fig. 3. Distribution of speed–accuracy correlations across experimental phases. Starting from the top three plots that represents a subject of the EF group, each colored dot identify a single trial, showing accuracy (expressed as the inverse of maximum error amplitude) plotted against maximum speed for that trial, in the launch phase. The axis limits are equal across all sub-plots. The area enclosed between the two exponential regression lines was defined as the *Improvement Area*. This area was computed only within the "SLOW" and "FAST" speed bounds (0.28 and 0.44 m/s, contained by the vertical dashed lines), speed ranges explicitly provided as feedback to the participants. A positive *Improvement Area* reflects enhanced accuracy (reduced error) relative to the preceding phase, while a negative value reflects a decline. Phase colors denote protocol stages: pre-Training force off, pre-Training force on, post-Training force on and post-Training force off. The lower panel shows violin plots of the calculated *Improvement Areas* for every participant, grouped by treatment (Error Fields [EF], Error Augmentation [EA], and Sham). The gray violins illustrate the change in *Improvement Area* when participants first encountered the curl force field relative to their baseline performance, reflecting the direct effects. The red violins indicate improvements achieved during practice with the EF force field (force-on trials), whereas the yellow violins capture improvements when practicing under EF exposure but assessed in force-off trials. Only the EF group exhibited negative values in the yellow condition, suggesting the presence of after-effects. Black horizontal and vertical bars denote statistically significant differences respectively with t-test and Kruskal-Wallis test using 95% confidence level: the vertical bars indicate statistical difference from zero, to test a significant change between the two phases analyzed, while the two horizontal bars indicate significant accuracy improvement for the EF and EA when compared to the SHAM group.

Interestingly we did not observe a significant difference in changes of error distributions when looking at practiced condition due to high variability of 3D movements; however we did detect significantly higher error levels in the post-training phases. In Figure 5 in unpracticed directions, EF group was most extreme. For the forces-on condition: (main effect of the group in Kruskal-Wallis $df = 2$, $F = 13.51$, $p = 0.00011$). EF has significantly 34 % higher than both EA ($p = 0.00014$, $CI = (12.75, 68.34)$) and 24.5 % higher than SHAM group ($p = 0.017$, $CI = (4.33, 59.92)$). EA and SHAM were not different ($p = 0.85$). For forces-OFF condition : (main effect of the group in Kruskal-Wallis $df = 2$, $F = 10.38$, $p = 0.0055$). EF was 22 % higher than both EA ($p = 0.0046$, $CI = (0.32, 55.92)$) and 29 % higher than SHAM group ($p = 0.0067$, $CI = (7.75, 63.33)$). EA and SHAM were not different ($p = 0.89$). Donchen, Shadmehr and others have found that generalization of learning from practiced to the unpracticed directions depends on their angular distance [33]–[35] and a angular distance of 90 degrees and above is destructive.

IV. Discussion

This study investigated an adaptive training paradigm for robot-assisted motor learning, emphasizing implicit learning that emerges through repeated reaching movements performed under externally applied force perturbations. At first, these perturbations interfered with the execution of the task, leading to larger movement errors in the reaching trajectories and reduced accuracy. However, such disturbances served as a stimulus for the motor control system, which gradually adapted to counteract external forces. With practice, participants exhibited progressively refined movement trajectories, reflecting improved control strategies. In line with the previous literature [36], the concept of motor adaptation refers to the process by which the nervous system continuously updates its internal model of the environment to mitigate the effects of perturbations. The approach specifically engages neural mechanisms to generate modified motor commands, recalibrate control processes, and enhance performance when exposed to force disturbances. This adaptive strategy effec-

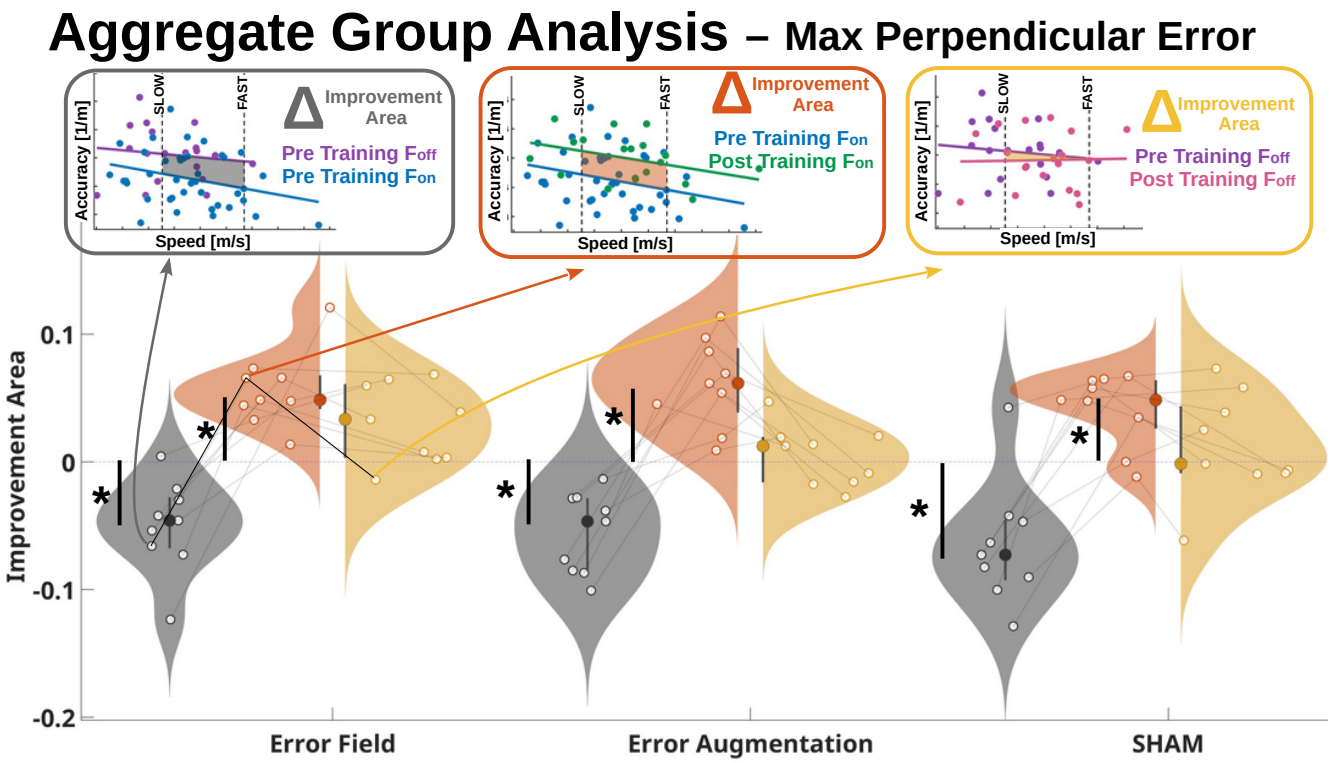

Fig. 4. Distribution of the *Improvement Area* obtained from the maximum perpendicular error for each subject separated by treatment group. Same approach as Fig. 3 but with a different metric. The zoom-in single subject analysis (the three scatter plots at the top) is the same subject analyzed in Fig. 3.

tively drives adjustments within the motor system, supporting improved outcomes in the reaching task, that can be visualized in the error tendencies. In this experiment, the improved outcomes are mostly evaluated in terms of the change in speed versus accuracy, as PM Fitts first hypothesized [37], where the accuracy is obtained as the inverse of the perpendicular error and error amplitude. Finally, these findings provided experimental validation for established theories of force-field adaptation and feedforward control [17], [19], [23], [38], extending them to the context of practical, robot-assisted rehabilitation protocols.

The Error Field force is our way to reprogram the subject's central nervous system connections, during a robotic practice, to improve the reaching task accuracy towards the ideal straight line trajectory. In neurotypical participants, is more challenging to induce a measurable motor improvement, as they do not initially have a big error to correct, unlike patients that suffer from a motor control deficit, like post-stroke or spinal cord injury, so what we focused on with our neurotypical population was a big initial error to start with, in order to see if a motor adaptation was induced throughout the experiment. We believe that a combination of Error Fields with the user's tailored experimental design [39], [40] will result in a more precise and efficient treatment dose with improved outcomes. Additionally, to make the neurotypical user condition more similar to the patient one, we immerse every subject to a velocity-dependent perturbation, the curl force field, that resembles the motor impairments found in a stroke-survivor population. What we found is that the Error Field group exhibited a bigger improvement after training with the force and this improvement was higher than the Error Augmentation group and the SHAM, but it resulted significantly different between groups only for the error amplitude metric, while it was significantly different from zero, in a per-group analysis, for both the metrics analyzed. The Error Augmentation group also did not demonstrate significant after-effects, suggesting in this case there was no change in the internal-model by the nervous system aimed at compensating for these perturbations [23], [38], but perhaps a different strategy used to cope with the disturbances such as increased co-contractions. These results leave some uncertainty about how subject variability may have influenced the outcomes and whether the chosen metrics best captured the motor improvements of interest. An interesting approach could be to analyze more errors relative to each subject's own baseline performance, as shown in Fig 5, rather than the ideal straight-line trajectory from start to target, to best identify how everyone improved from their own self. Additionally, the assumption of normality in the error distributions used to generate the Error Fields might be improved by additional Gaussian components, to compensate for the asymmetries, and ideal Error Fields update every N trials as the subject progresses through the training, following [17]. Another limitation lies in the 3D reaching task projected onto a 2D screen (even if equipped with stereoscopic imaging), where reduced depth perception likely introduced visual

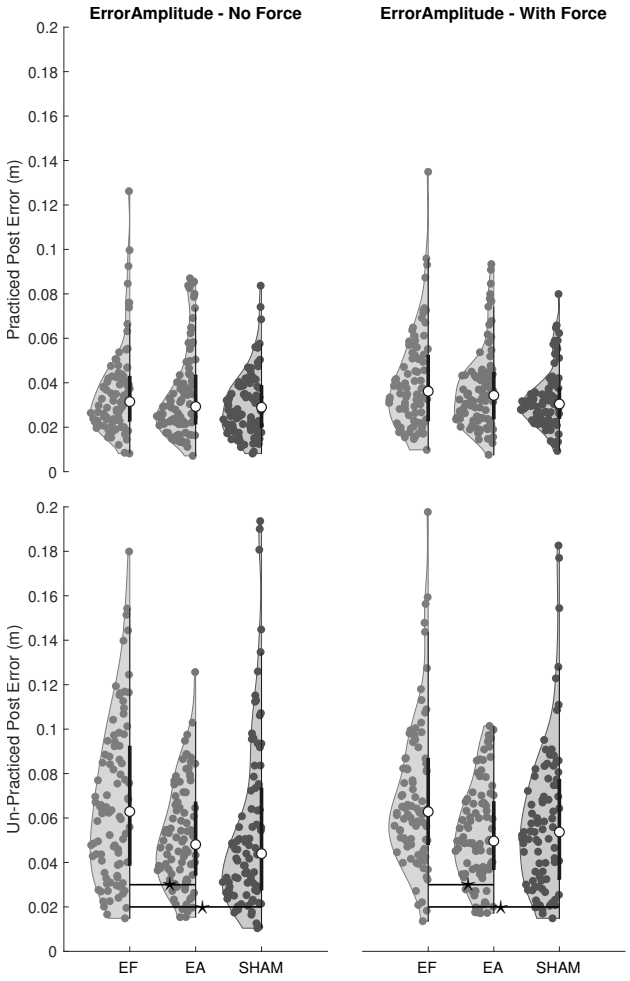

Fig. 5. Post-Training error amplitude in practiced and unpracticed conditions, compared to the pre-Training force off distributions, for each direction. EF group had more to learn and hence had increased error in unpracticed phases supporting the argument of generalization.

uncertainty, adding complexity to the experiment and noise to the recorded trajectories. Additionally, the robotic arm used for the experiment is not equipped with a force sensor and so it was not possible to determine the exact force applied to the subject's hand at every instant, but we had to rely on the internal kinematic models of its controller, and we experimentally measured with an external force sensor the difference between the desired force and the actual generated force at the end effector for multiple directions, and the discrepancies were lower than 5%.

APPENDIX A

To calculate errors, we first transformed the robot end-effector position $\mathbf{x}(\delta)$, where δ is path distance originally described in the left-handed Unity reference frame $[U]$, into the right-handed frame $[i]$ associated with movement direction d_i (Fig.6). The origin of frame $[i]$ is fixed at the ideal start position $\mathbf{x}_S$, and its x-axis points towards the target $\mathbf{x}_T$. The homogeneous transformation is defined as:

$$\rho_i(\delta) = T_{iU}\,\mathbf{x}(\delta)$$

where T_{iU} consists of a rotation R_{iU} and a translation $\mathbf{p}_{iU}$, shown below.

$$T_{iU} = \begin{bmatrix} \mathrm{R}_{iU} & \mathbf{p}_{iU} \\ \mathbf{0}^\top & 1 \end{bmatrix}$$

$$\mathrm{R}_{iU} = \begin{bmatrix} \mathrm{d}_i & -\langle \mathrm{d}_i \times \mathrm{g} \rangle & \langle (-\mathrm{d}_i \times \mathrm{g}) \times \mathrm{d}_i \rangle \end{bmatrix}^\top$$

$$\mathbf{p}_{iU} = -\mathbf{x}_S$$

where g is the gravity vector expressed in $[U]$, $\langle \cdot \rangle$ denotes normalization to a unit vector, $\times$ is the cross product operator, and $^\top$ indicates the transpose.

The second and third components of the transformed position vector $\rho_i(\delta)$ correspond to the horizontal and vertical errors, respectively. To calculate the extent error $\mathbf{e}_{ext}(\delta)$, we strapped origin of $[E]$ (Fig. 6) to the ideal hand position $x_{MJ}(\delta)$, given by the minimum-jerk trajectory.

$$\mathbf{e}(\delta) = \begin{bmatrix} \mathbf{e}_{ext}(\delta) \\ \mathbf{e}_{hor}(\delta) \\ \mathbf{e}_{ver}(\delta) \end{bmatrix} = \begin{bmatrix} \mathrm{I} & \mathbf{p}_{Ei}(\delta) \\ \mathbf{0}^\top & 1 \end{bmatrix} \rho_i(\delta) = T_{Ei}(\delta) T_{iU} \mathbf{x}(\delta)$$

where:

$$\mathbf{p}_{Ei}(\delta) = \begin{bmatrix} -x_{MJ}(\delta) \\ 0 \\ 0 \end{bmatrix}$$

An ideal trajectory in $[U]$ follows a minimum-jerk profile along the straight line connecting the start position $\mathbf{x}_S$ to the target $\mathbf{x}_T$ (orange trace in Fig.6). When expressed in $[i]$, this trajectory progresses along the x-axis from 0 to 0.1 according to $x_{MJ}(\delta)$. However, in the error frame $[E]$, the same ideal trajectory remains stationary at the origin.

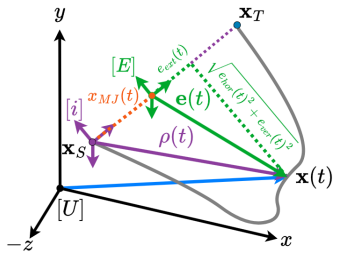

Fig. 6. Positions, reference frames and error vector used to calculate all the variables and parameters in the reaching trial space (from start position Xs to target position Xt).

ACKNOWLEDGMENT

The authors would like to express their gratitude to the Robotics Lab at Shirley Ryan AbilityLab and to the Richard and Loan Hill Department of Biomedical Engineering at the University of Illinois Chicago for their support. The generative Open AI model ChatGPT has been used to create a cartoon version from a real image in Fig. 1 A. The authors declare that they have no conflicts of interest, financial or otherwise.

REFERENCES

[1] X. Li, Y. He, D. Wang, and M. J. Rezaei, "Stroke rehabilitation: from diagnosis to therapy," *Frontiers in neurology*, vol. 15, p. 1402729, 2024.

[2] D. J. Lin, S. P. Finklestein, and S. C. Cramer, "New directions in treatments targeting stroke recovery," *Stroke*, vol. 49, no. 12, pp. 3107–3114, 2018.

[3] S. Tesfazgi, A. Lederer, J. F. Kunz, A. J. Ordóñez-Conejo, and S. Hirche, "Personalized rehabilitation robotics based on online learning control," *arXiv preprint arXiv:2110.00481*, 2021.

[4] L. Masia, M. Casadio, P. Giannoni, G. Sandini, and P. Morasso, "Performance adaptive training control strategy for recovering wrist movements in stroke patients: a preliminary, feasibility study," *Journal of neuroengineering and rehabilitation*, vol. 6, no. 1, p. 44, 2009.

[5] V. Klamroth-Marganska, J. Blanco, K. Campen, A. Curt, V. Dietz, T. Ettlin, M. Felder, B. Fellinghauer, M. Guidali, A. Kollmar *et al.*, "Three-dimensional, task-specific robot therapy of the arm after stroke: a multicentre, parallel-group randomised trial," *The Lancet Neurology*, vol. 13, no. 2, pp. 159–166, 2014.

[6] S. Dalla Gasperina, V. Longatelli, M. Panzenbeck, B. Luciani, A. Morosini, A. Piantoni, P. Tropea, F. Braghin, A. Pedrocchi, and M. Gandolla, "Agree: an upper-limb robotic platform for personalized rehabilitation, concept and clinical study design," in *2022 International Conference on Rehabilitation Robotics (ICORR)*. IEEE, 2022, pp. 1–6.

[7] N. J. Schork, "Personalized medicine: time for one-person trials," *Nature*, vol. 520, no. 7549, pp. 609–611, 2015.

[8] G. S. Ginsburg and H. F. Willard, "Genomic and personalized medicine: foundations and applications," *Translational research*, vol. 154, no. 6, pp. 277–287, 2009.

[9] M. A. Hamburg and F. S. Collins, "The path to personalized medicine," *New England Journal of Medicine*, vol. 363, no. 4, pp. 301–304, 2010.

[10] M. K. Marko, A. M. Haith, M. D. Harran, and R. Shadmehr, "Sensitivity to prediction error in reach adaptation," *Journal of neurophysiology*, vol. 108, no. 6, pp. 1752–1763, 2012.

[11] Y. Wei, P. Bajaj, R. Scheidt, and J. Patton, "Visual error augmentation for enhancing motor learning and rehabilitative relearning," in *9th International Conference on Rehabilitation Robotics, 2005. ICORR 2005.* IEEE, 2005, pp. 505–510.

[12] K. Takiyama, M. Hirashima, and D. Nozaki, "Prospective errors determine motor learning," *Nature communications*, vol. 6, no. 1, p. 5925, 2015.

[13] D. J. Herzfeld, P. A. Vaswani, M. K. Marko, and R. Shadmehr, "A memory of errors in sensorimotor learning," *Science*, vol. 345, no. 6202, pp. 1349–1353, 2014.

[14] J. L. Patton, M. E. Stoykov, M. Kovic, and F. A. Mussa-Ivaldi, "Evaluation of robotic training forces that either enhance or reduce error in chronic hemiparetic stroke survivors," *Experimental brain research*, vol. 168, no. 3, pp. 368–383, 2006.

[15] F. Abdollahi, S. V. Rozario, R. V. Kenyon, J. L. Patton, E. Case, M. Kovic, and M. Listenberger, "Arm control recovery enhanced by error augmentation," in *2011 IEEE International Conference on Rehabilitation Robotics*. IEEE, 2011, pp. 1–6.

[16] F. Abdollahi, E. D. Case Lazarro, M. Listenberger, R. V. Kenyon, M. Kovic, R. A. Bogey, D. Hedeker, B. D. Jovanovic, and J. L. Patton, "Error augmentation enhancing arm recovery in individuals with chronic stroke: a randomized crossover design," *Neurorehabilitation and neural repair*, vol. 28, no. 2, pp. 120–128, 2014.

[17] N. R. Aghamohammadi, M. F. Bittmann, V. Klamroth-Marganska, R. Riener, F. C. Huang, and J. L. Patton, "Error fields: personalized robotic movement training that augments one's more likely mistakes," *Scientific Reports*, vol. 15, no. 1, p. 4201, 2025.

[18] M. E. Fisher, F. C. Huang, V. Klamroth-Marganska, R. Riener, and J. L. Patton, "Haptic error fields for robotic training," in *2015 IEEE world haptics conference (WHC)*. IEEE, 2015, pp. 434–439.

[19] B. Borghi, N. R. Aghamohammadi, A. Cancrini, A. Ramirez, C. Celian, and J. Patton, "Personalized robotic training on a planar reaching task," in *2025 International Conference On Rehabilitation Robotics (ICORR)*. IEEE, 2025, pp. 1493–1499.

[20] R. J. Van Beers, P. Haggard, and D. M. Wolpert, "The role of execution noise in movement variability," *Journal of neurophysiology*, vol. 91, no. 2, pp. 1050–1063, 2004.

[21] K. Sutter, L. Oostwoud Wijdenes, R. J. van Beers, and W. P. Medendorp, "Movement preparation time determines movement variability," *Journal of Neurophysiology*, vol. 125, no. 6, pp. 2375–2383, 2021.

[22] A. J. Westerveld, A. C. Schouten, P. H. Veltink, and H. van der Kooij, "Passive reach and grasp with functional electrical stimulation and robotic arm support," in *2014 36th annual international conference of the IEEE engineering in medicine and biology society*. IEEE, 2014, pp. 3085–3089.

[23] R. Shadmehr and F. A. Mussa-Ivaldi, "Adaptive representation of dynamics during learning of a motor task," *Journal of neuroscience*, vol. 14, no. 5, pp. 3208–3224, 1994.

[24] W. T. Townsend, D. Wilkinson, A. Jenko, J. Leland, A. Ananthanarayanan, and J. Patton, "Multi-active-axis, non-exoskeletal rehabilitation device," Nov. 20 2018, uS Patent 10,130,546.

[25] T. Ishida and A. Takanishi, "A robot actuator development with high backdrivability," in *2006 IEEE Conference on Robotics, Automation and Mechatronics*. IEEE, 2006, pp. 1–6.

[26] J. J. Patton, "New vr technologies for sensorimotor rehabilitation," *Transactions of Japanese Society for Medical and Biological Engineering*, vol. 51, no. Supplement, pp. M–99, 2013.

[27] F. Porta, C. Celian, and J. L. Patton, "Upper extremity functional rehabilitation for stroke survivors using error-augmented visual feedback: interim results," in *2021 43rd Annual International Conference of the IEEE Engineering in Medicine & Biology Society (EMBC)*. IEEE, 2021, pp. 1318–1324.

[28] C. Celian, M. Verardi, and J. Patton, "Visual error augmentation during bimanual therapy in individuals post stroke," *Archives of Physical Medicine and Rehabilitation*, vol. 103, no. 12, p. e91, 2022.

[29] B. L. Schwartz and J. H. Krantz, *Sensation and perception*. Sage Publications, 2018.

[30] N. R. Aghamohammadi, C. Celian, V. Wojcik, B. Borghi, A. Ramirez, A. Cancrini, and J. L. Patton, "A case study of error fields: A three-dimensional personalized robotic therapy," in *2025 International Conference On Rehabilitation Robotics (ICORR)*. IEEE, 2025, pp. 1485–1492.

[31] T. Flash and N. Hogan, "The coordination of arm movements: an experimentally confirmed mathematical model," *Journal of neuroscience*, vol. 5, no. 7, pp. 1688–1703, 1985.

[32] R. Shadmehr and S. P. Wise, *The computational neurobiology of reaching and pointing: a foundation for motor learning*. MIT press, 2004.

[33] O. Donchin, J. T. Francis, and R. Shadmehr, "Quantifying generalization from trial-by-trial behavior of adaptive systems that learn with basis functions: theory and experiments in human motor control," *Journal of Neuroscience*, vol. 23, no. 27, pp. 9032–9045, 2003.

[34] J. W. Krakauer, P. Mazzoni, A. Ghazizadeh, R. Ravindran, and R. Shadmehr, "Generalization of motor learning depends on the history of prior action," *PLoS biology*, vol. 4, no. 10, p. e316, 2006.

[35] J. L. Patton, Y. J. Wei, P. Bajaj, and R. A. Scheidt, "Visuomotor learning enhanced by augmenting instantaneous trajectory error feedback during reaching," *PloS one*, vol. 8, no. 1, p. e46466, 2013.

[36] F. Gandolfo, F. A. Mussa-Ivaldi, and E. Bizzi, "Motor learning by field approximation." *Proceedings of the National Academy of Sciences*, vol. 93, no. 9, pp. 3843–3846, 1996.

[37] P. M. Fitts, "Cognitive aspects of information processing: Iii. set for speed versus accuracy." *Journal of experimental psychology*, vol. 71, no. 6, p. 849, 1966.

[38] J. L. Patton and F. A. Mussa-Ivaldi, "Robot-assisted adaptive training: custom force fields for teaching movement patterns," *IEEE Transactions on Biomedical Engineering*, vol. 51, no. 4, p. 636–646, 2004.

[39] A. Cancrini, B. Borghi, N. R. Aghamohammadi, A. Ramirez, C. Celian, and J. L. Patton, "Prism: Parameter recovery identification from synthetic modeling," in *2025 International Conference On Rehabilitation Robotics (ICORR)*. IEEE, 2025, pp. 1396–1402.

[40] A. Cancrini, B. Borghi, N. R. Aghamohammadi, A. Ramirez, and J. L. Patton, "Defining experimental design for human motor control identification: A novel framework," *IEEE Transactions on Neural Systems and Rehabilitation Engineering*, 2026.